Received: 12 July 2020 | Revised: 18 March 2021 | Accepted: 25 March 2021

DOI: 10.1002/pc.26057

RESEARCH ARTICLE

Polymer COMPOSITES WILEY

Comparative studies of silane coupled e-glass fiber and e-glass fiber reinforced bismaleimide-epoxy hydroxylated $BaTiO_3$ nanocomposites on the dielectric and mechanical properties

Savitha Unnikrishnan K. | **Sunil Jose T.** | **Dinoop lal S.**

Research and PG Department of Chemistry, St. Thomas' College (Affiliated to University of Calicut), Thrissur, Kerala, India

Correspondence
Sunil Jose T., Research and PG Department of Chemistry, St.Thomas' College (Autonomous), Thrissur 680 001, Kerala, India.
Email: suniljosestc@gmail.com; sjtppc@gmail.com

Abstract

Silane coupled E-glass fiber (SC-EGF) and E-glass fiber (EGF) reinforced bismaleimide (BMI)-epoxy-hydroxylated $BaTiO_3$ (BTOH) nanocomposites with 1–5 wt% of BTOH nanofiller were fabricated by hand lay-up method and compression molded. Surface hydroxylation of synthesized $BaTiO_3$ nanoparticles was carried out using H_2O_2. Both BT and BTOH nanoparticles were characterized by SEM, XRD, and FTIR studies. Among the reinforced nanocomposites, SC-EGF-reinforced showed a remarkable increase in mechanical and dielectric properties. The tensile strength of BMI-epoxy composite increased 1.56 and 3.10 times when loaded with 2 and 3 wt% of BTOH, respectively. Their flexural strength too increased 2.14 and 2.21 times upon 2 and 3 wt% of BTOH loading. BMI-epoxy-BTOH nanocomposites with 3 wt% of BTOH showed higher tensile strength, flexural strength, and dielectric strength indicating that it possesses better mechanical and insulating properties and composites with 2 wt% showed higher dielectric constant and lower dielectric loss indicating that this composition could be explored to high dielectric applications.

KEYWORDS

bismaleimide, dielectric strength, hydroxylated $BaTiO_3$

1 | INTRODUCTION

Due to the significant improvements in electrical and mechanical properties, polymer nanocomposites have widespread applications in energy storage and microelectronic devices, sensors and so forth. Bismaleimide (BMI) resin is an young and leading class of thermosetting polyimide and this high-performance resin find application in spaceware composites, radar, capacitors, stealth technologies, printed circuit board (PCB) etc.[1] They possess excellent oxidative stability, rigidity, thermo-mechanical properties, inferior moisture absorption, high glass transition temperature, highest service temperature capability, and retention of physical properties at elevated temperatures as well as in wet conditions. To overcome the brittleness and to improve the processability, BMI resin is blended with epoxy resin. Epoxy resins are used as matrix resins in aerospace composites because of its easy processing, handling convenience, excellent mechanical properties, and adhesive nature. Epoxy resins can only be used safely around 140°C because of their low glass transition temperatures.[2] Due to poor hot/wet performance and high moisture sensitivity, they are not used for applications at high-temperature conditions. So, blending of BMI with epoxy will be attractive if it results in a matrix with beneficial characteristics of the two constituents.

High dielectric permittivity (k) materials have widespread applications in various fields like energy storage capacitors, microcapacitors, sensors, and printed circuit boards. Incorporation of high-k nanofillers into the polymer matrix leads to an increase in the dielectric constant of the polymer nanocomposites. Among the dielectric ceramic particles like barium titanate (BT), barium strontium titanate, boron nitride, and lead zirconate titanate, BT exhibits high dielectric constant and has widespread applications.

Usually, ferroelectric nanoceramics like BT have poor compatibility with the polymer matrix because of their small size and high surface energy; they are more susceptible to aggregation leading to lowering of dielectric breakdown due to increase in leakage current. Surface functionalization of the filler was the currently employed technique to overcome this problem. Many research based on the surface modification of the nanofiller were carried out not only to enhance the dielectric properties of the polymer nanocomposites but also to improve the compatibility with the polymer matrix.

There are so many ways to modify the surface of BT nanoparticles such as hydroxylation by H_2O_2,[3–8] silanization using different silane coupling agents,[9–11] dopamine modification,[12] 2,3,4,5-tetra fluorobenzoic acid,[13] fluorinated phosphonic acid modification,[14] modification with nonionic and hydrophilic surface agent like polyethylene glycol,[15] surface aminated BT nanoparticles,[16] chemical modification of the hydroxylated BT nanoparticles using titanate coupling agents,[17] modification by ligand exchange reactions,[18] by palmitic acid,[19] and by sodium oleate.[20,21] The nanocomposites embedded with these surface hydroxylated and chemically modified nanofillers and nanofibers exhibited remarkable improvement in the dielectric properties, which may be ascribed to the enhanced interfacial interaction between the nanoparticles and the polymer matrix, thereby increasing the uniform dispersion of nanoparticles with reduced agglomeration. These nanocomposites also exhibit high dielectric permittivity, breakdown strength, low dielectric loss, and good compatibility.

Among the various chemical modification processes, silanization using silane coupling agents is the most accepted method because further activation of the particle surface can be done by introducing different functional groups into it. The silane coupling agents are usually added to surface hydroxylated BT nanoparticles (BTOH) because they are more prone to silanization than BT because of the polarity of the former. Current researches reveal that silanization of nanoparticles strongly depends on the reaction kinetics such as reaction time, temperature, different silane coupling agents, and solvent effects.

In the present work, surface modification of hydrothermally synthesized BT nanoparticles was carried out by hydroxylation using H_2O_2 treatment. It is the simplest and easiest method for surface modification compared to silanization. The interfacial dipole layer emerged from the surface hydroxylated BT particles portrays a significant role in the dielectric properties of the fabricated BMI-epoxy composites. As BT lacks reactive functional groups, modification using organic reagents only leads to physisorption on the nanoparticles either by the electrostatic force of attraction or by van der Waal's forces. The synthesized BT nanoparticles contain a low concentration of surface hydroxyl groups, and this will not significantly improve the surface activity. For effective modification of BT, many hydroxyl groups are to be produced on the surface of BT nanoparticles that can be attained by treating BT with H_2O_2. Glass fibers were introduced to the BMI-epoxy resin matrix via hand lay-up method to improve the mechanical properties of the polymer nanocomposites.

2 | MATERIALS AND EXPERIMENTAL

2.1 | Materials

BMI resin was supplied by ABROL, Hyderabad. Commercial epoxy resin, Epofine-1564 was purchased from SME Business Services Ltd., Maharashtra and E-glass fibers from Urja Products, Ahmedabad, India. $Ti(C_4H_9O)_4$, $Ba(OH)_2{\cdot}8H_2O$, and H_2O_2 were purchased from Sigma–Aldrich and HNO_3 from Merck, India.

2.2 | Synthesis of barium titanate nanoparticles and hydroxylated barium titanate nanoparticles

$BaTiO_3$ nanoparticles were synthesized using tetrabutyltitanate and barium hydroxide octahydrate as precursors by employing hydrothermal method.[22–26] One milliliter of tetrabutyltitanate was dissolved in 18 mL ethanol solution with constant stirring. To this mixture, a solution containing 0.06 mL HNO_3 and 3 mL distilled water was added slowly. Ten milliliter of this solution was then added in drops into 1 M aqueous barium hydroxide with continuous stirring. This mixture was treated at 200°C for 16 h in an autoclave lined with Teflon. After filtration, the obtained products were washed with a mixture of ethanol-distilled water and then dried at 60°C for 24 h under vacuum.[27] Modification of the surface of the synthesized BT nanoparticles

was done by treating the BT nanoparticles with H_2O_2. First, the BT nanoparticles and H_2O_2 mixture were ultrasonicated for half an hour. After sonication, the mixture was heated up to 106°C and continued heating for 5 h and finally, the obtained hydroxylated barium titanate nanoparticles (BTOH) were filtered and dried at 60°C for 19 h.[6] Schematic representation of the synthesis route is given in Figure 1.

2.3 | Fabrication of BMI-epoxy composites

Both silane coupled E-glass fiber (SC-EGF) and E-glass fiber (EGF) reinforced BMI-epoxy composites with 1–5 wt % of BTOH nanofiller and without this, nanofiller was fabricated using hand lay-up method followed by compression molding.[28] Here, the BMI epoxy resin weight ratio was maintained at 15:1.5 in all the composites.

2.4 | Characterization

The chemical structure of the BMI resin, BMI-epoxy composites, BT nanoparticles, BTOH nanoparticles, and interactions of the BTOH nanoparticles in the polymer nanocomposites were characterized using Fourier transform Infrared Spectroscopy (FTIR), IR Affinity-1S, Shimadzu, Japan. Powder X-ray diffraction (XRD) patterns of the synthesized BT and BTOH nanoparticles, BMI-epoxy composite without BTOH nanoparticles, BMI-epoxy nanocomposites with varying percentages of BTOH nanoparticles using X-ray diffractometer Aeris, and PANalytical with Copper-K alpha radiation (1.5406A° wavelength) as the source were obtained at room temperature. The scanning angle was set in the range of 5°–80°. The morphological studies of BMI resin, BTOH nanoparticles, BMI-epoxy composite without BTOH nanofiller, and BMI-epoxy composite with 2%wt of the BTOH nanoparticles were done using the scanning electron microscope (SEM) images from JSM-6390LV. Elemental characterization of BTOH nanoparticles and BMI-epoxy composites with 3 wt% of BTOH nanoparticles were assessed by Energy dispersive X-ray analysis using Jeol 6390LA/OXFORD XMX N. TEM analysis of BMI-epoxy composites with 3 wt% of BTOH nanoparticles without EGF were done using Jeol/JEM 2100.The flexural and tensile tests of the composites were measured as per ASTM standards using the universal testing machine, Autograph AG-X plus, Shimadzu. Dielectric behavior of the samples was studied in the frequency range of 10^2–10^7 Hz using LCR meter as per ASTM standards, the dielectric break down strength were measured using Hipotronics AC Dielectric test set.

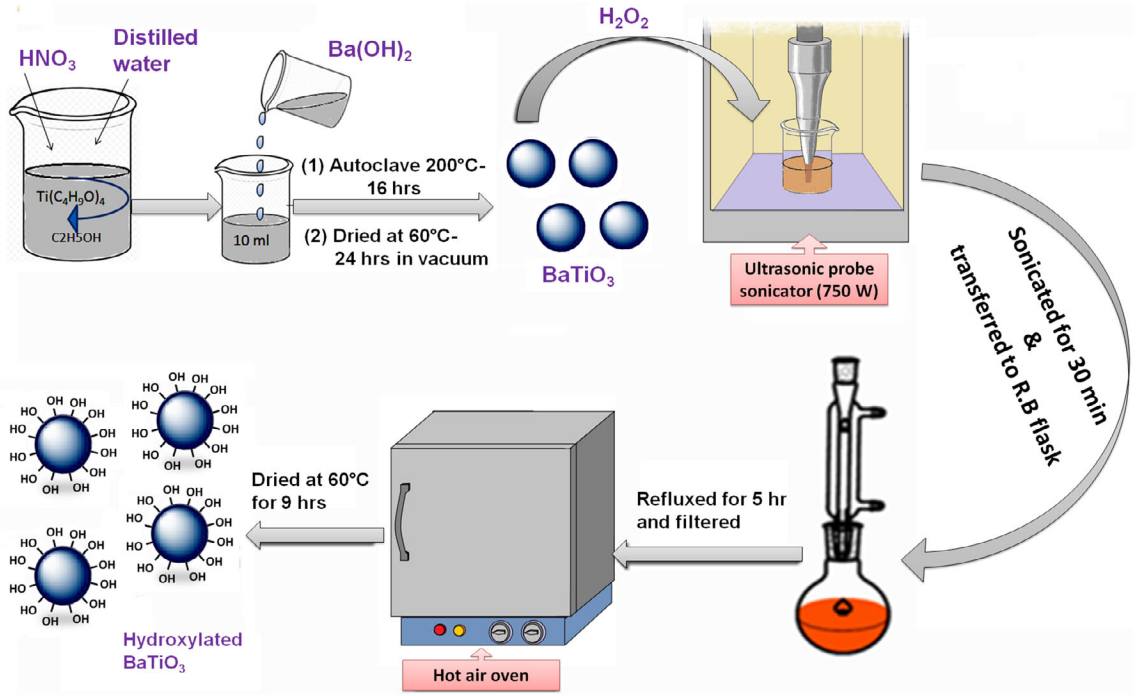

FIGURE 1 Preparation of $BaTiO_3$ (barium titanate [BT]) and surface hydroxylated $BaTiO_3$ (BTOH) nanoparticles [Color figure can be viewed at wileyonlinelibrary.com]

3 | RESULTS AND DISCUSSION

3.1 | Fourier transform infrared spectra analysis

Fourier transform infrared spectra of the synthesized $BaTiO_3$ and surface hydroxylated $BaTiO_3$ nanoparticles were illustrated in Figure 2. The absorptions at 637 cm^{-1} in $BaTiO_3$ and 645 cm^{-1} in surface hydroxylated $BaTiO_3$ nanoparticles correspond to metal-oxygen (Ti—O) stretching vibrations. Absorptions at 1641 and 3411 cm^{-1} correspond to the —OH deformations and stretching vibrations, respectively, establishing the presence of adsorbed —OH group. A strong peak around 1436 cm^{-1} in both spectra corresponds to C—O stretching vibrations arose from the carbonate impurity, which is present as $BaCO_3$ in trace quantities along with $BaTiO_3$ during the hydrothermal synthesis of $BaTiO_3$.[29] Broadband in the range of 3000–3700 cm^{-1} corresponds to —OH stretching vibrations, which confirms the presence of effectively surface hydroxylated BT nanoparticles. The characteristic absorption at 868 cm^{-1} corresponds to barium–oxygen bond in BT particles.[15,30]

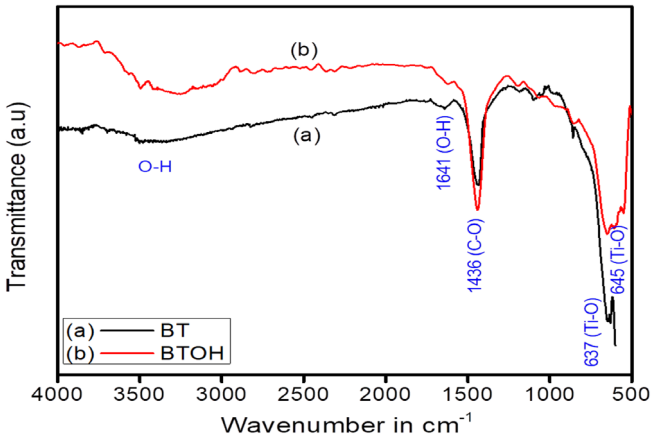

FIGURE 2 FTIR spectra of the synthesized (A) BaTiO3 (barium titanate [BT]) (B) hydroxylated $BaTiO_3$ (BT-OH) nanoparticle [Color figure can be viewed at wileyonlinelibrary.com]

FTIR spectra of EGF and SC-EGF reinforced BMI-epoxy composites with BTOH loadings in the range from 1 to 5 wt% are illustrated in Figure 3. A thorough analysis of the spectra throws light into the fact that the characteristic absorptions are retained in both the spectra. Analysis of the spectra reveals that the absorption bands correspond to (i) the maleimide ring and imide group at 686— and 1387 cm^{-1}, (ii) benzene ring at 820 cm^{-1}, (iii) C—N—C maleimide group around 1100 cm^{-1}, (iv) weak C—N stretch around 1020 cm^{-1}, (v) C═O group at 1710 cm^{-10}, and (vi) C═C of benzene ring at 1510 cm^{-1}. The absence of epoxide ring absorption bands at 915, 970, 862, and 1248 cm^{-1} in BMI-epoxy nanocomposites indicates that there exists an intercrosslinking between BMI and epoxy resin, which occurs through the oxirane ring opening of the epoxy resin (refer supporting information Figure S1). Absorption at 2965 cm^{-1} corresponding to CH stretching vibration of BMI-Epoxy composite without nanofiller is very much reduced in BMI-epoxy composite with BTOH nanofiller. Also absorption at 1386 cm^{-1} corresponds to CH_2 vibrational wagging shifts to lower wavenumber. Both these observations pointed out the possibility of hydrogen bonding between the CH_2 hydrogen atoms of BMI-epoxy matrix with oxygen atoms of surface hydroxylated BTOH

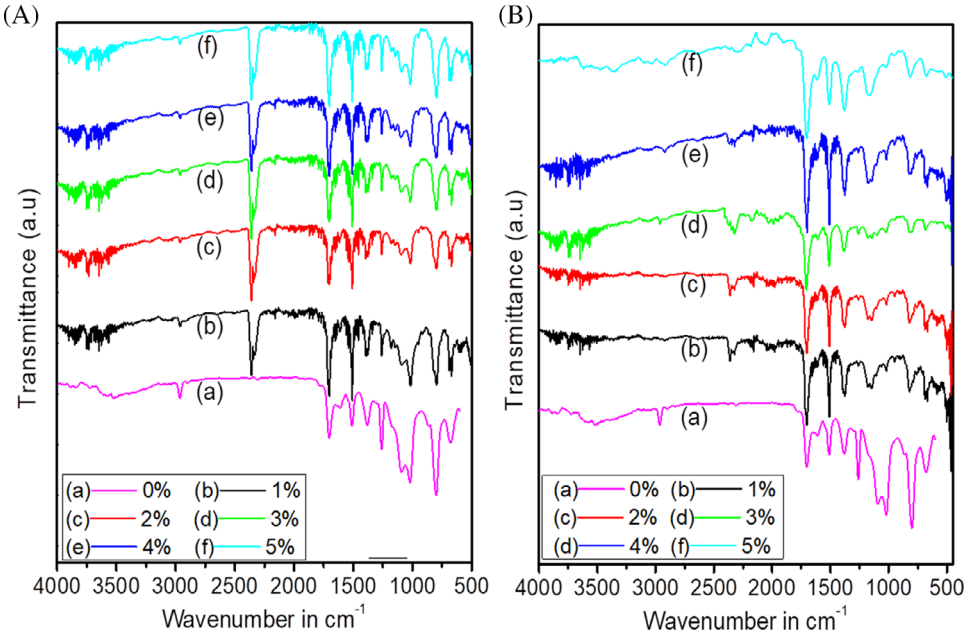

FIGURE 3 FTIR spectra of (A) E-glass fiber (EGF) reinforced and (B) silane coupled E-glass fiber (SC-EGF) reinforced bismaleimide (BMI)-epoxy-BTOH nanocomposites [Color figure can be viewed at wileyonlinelibrary.com]

nanofiller. Each composite also exhibiting broadband in the range of 3000–3700 cm^{-1} indicates the presence of surface hydroxylated BT nanoparticles.

3.2 | Powder X-ray diffraction analysis

The perovskite cubic phase of the synthesized BT (Figure 4(A)) was confirmed by XRD analysis and the peaks at 2θ = 22.19(100), 31.57(110), 38.92(111), 45.27 (200), 50.96(210), 56.18(211), 65.87(220), 70.39(300), 74.82 (310), and 79.17(311) were more consistent with the reported data with JCPDS No#892475.

From X-ray diffractograms of both BT and BTOH nanoparticles, at 2θ values around 31.6°, the most intense peak (110) were observed. The single peak at 2θ = 45.13° and 45.23° for BT and BTOH nanoparticles, respectively, again confirms the presence of perovskite cubic phase of BT and BTOH.[31] These single peaks without splitting can be used to distinguish the cubic phase from the tetragonal phase of BT because the latter has two overlapping or close peaks at 44.85° and 45.38° in XRD patterns.[32–34]

From Figure 4, it is clear that there is no change in the XRD patterns of BT and BTOH which indicates that even after refluxing BT nanoparticles with H_2O_2 for 19 h, crystallization of only BT nanoparticles remained with no other crystalline byproducts. Based on the XPS data and zeta potential values, Ohia Chen Li et al. concluded that during surface hydroxylation of BT nanoparticles, the —OH is attached to barium instead of titanium and this causes the surface of hydroxylated BT to be more Bronsted basic that may be attributed from the lower ionic potential of barium compared to titanium.[6] H_2O_2 is an oxidizing agent and it reduces oxygen to OH, only oxygen atoms present at the surface are reduced to OH, whereas that present in the bulk remains as such without undergoing reduction[7]. Comparison of FTIR spectra of BT and BTOH further supports the surface hydroxylation argument. The bands corresponding to Ba—O vibrations (868 cm^{-1}) were less intense in the spectra of BTOH, whereas more intense O—H stretching vibrations (3700–3000 cm^{-1}) could be observed in BTOH compared to BT. The average crystallite size of the BT and BTOH nanoparticles is calculated using Scherrer's formula and is found to be 33 and 28 nm, respectively.

The incorporation of BT-OH nanofiller to BMI-epoxy resin resulted in no significant shift in the position of the intense peaks at 2θ = 19°–22°. Sharp crystal peaks corresponding to BT-OH nanoparticles were seen in the XRD patterns of the composites. Further analysis of Figure 5 reveals that the most intense peak of BT-OH nanofiller at 2θ value around 32° is retained along with peaks corresponding to the perovskite cubic structure at 2θ value around 45.5° indicating that there is effective dispersion of BT-OH nanofiller in the BMI-epoxy matrix.[35]

3.3 | Morphological studies of BMI-epoxy nanocomposites

SEM images reveal the morphology of BTOH (Figure 6 (A)), BMI resin (refer supporting information Figure S2 A), BMI-epoxy composites with (Figure 6(B))

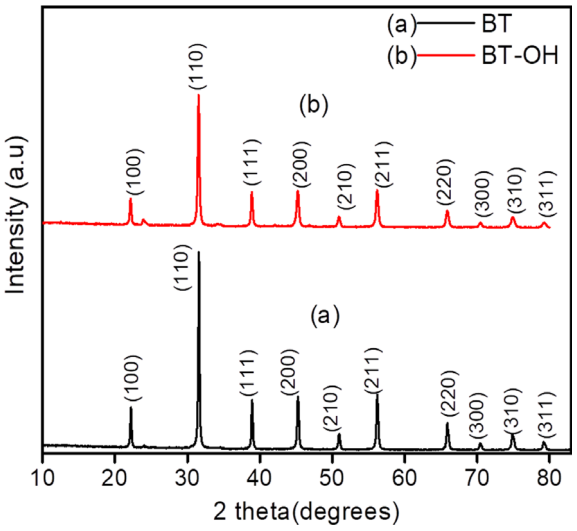

FIGURE 4 Powder XRD patterns of (A) barium titanate (BT) nanoparticles (B) BTOH nanoparticles [Color figure can be viewed at wileyonlinelibrary.com]

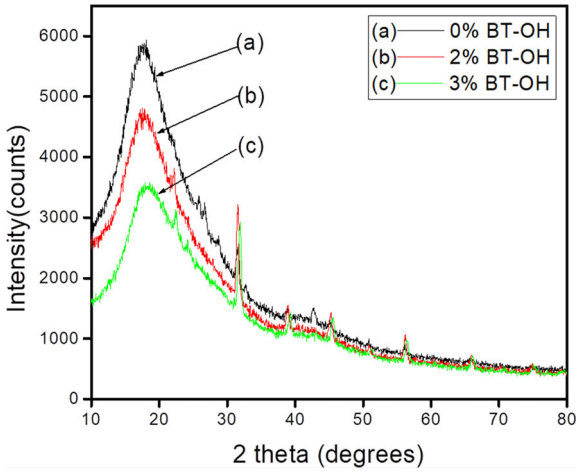

FIGURE 5 Powder XRD patterns of (A) bismaleimide (BMI)-epoxy composite without BTOH nanofiller and BMI-epoxy composites with (B) 2% and (C) 3% BTOH nanofiller [Color figure can be viewed at wileyonlinelibrary.com]

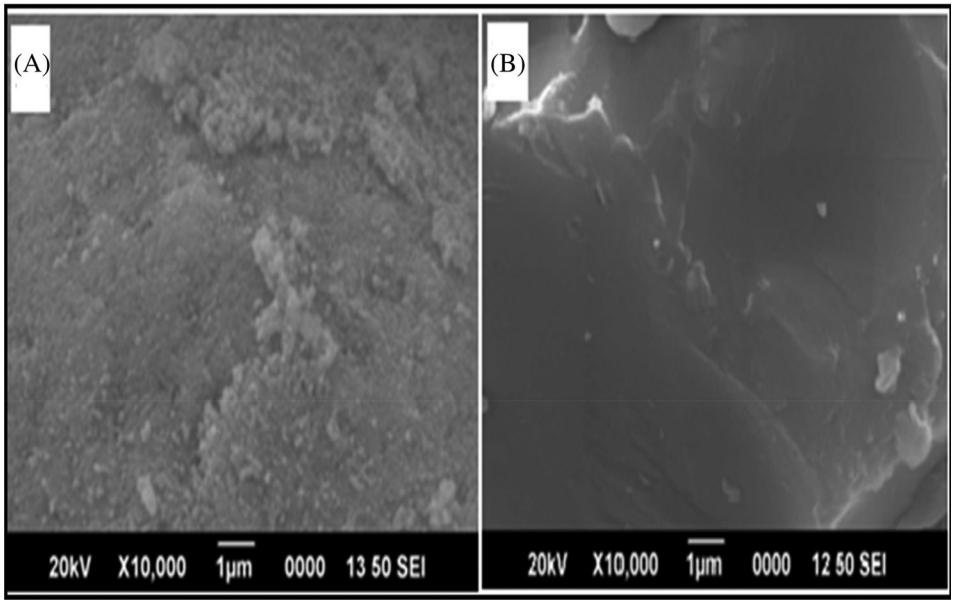

FIGURE 6 SEM images of (A) BTOH nanoparticle (B) bismaleimide epoxy composite with 2% BTOH

and without (refer supporting information Figure S2 B) BTOH nanocomposites. EDAX analysis of the synthesized BTOH nanoparticles (refer supporting information Figure S3) confirmed that there were no impurities in the sample with a quantitative composition of barium ≈ 65%, titanium ≈ 17%, and oxygen ≈ 18%. EDAX spectra and mapping images of the synthesized BMI-epoxy composites with 3 wt% of BTOH nanoparticles showed the presence of elements carbon, oxygen, barium, and titanium with their dispersion in the composite matrix (refer supporting information Figure S4). The presence of chlorine atom in traces, as impurity, observed in the spectra of composite might have originated from the BMI since the EDAX of BTOH is free of chlorine (refer supporting information Figure S3). The EDAX pattern hence shows the presence of all the elements as expected, for BMI-epoxy BTOH composites.

Figure 6(B) represents the cross-sectional SEM image of BMI-epoxy nanocomposite loaded with 2 wt% of BTOH nanoparticles and it reveals a uniform smooth surface of nanocomposite with no folding over or buckling. The phase of embedded BTOH nanoparticle is not that much visible in the polymer matrix, which is identifiable as the dark gray region.

Transmission electron microscope (TEM) and selected area electron diffraction (SAED) images were also taken, in order to study the dispersion of BTOH in BMI-epoxy composites with 3 wt% of BTOH nanoparticles without EGF reinforcement. From the figure (supporting information Figure S5 A, B, and C), it is evident that BTOH nanoparticles were homogeneously distributed without any agglomeration. The brighter spherical parts may indicate glass fibers, which were unknowingly present during the powdering of the sample. SAED pattern of the composite showed no clear spots or distinct ring patterns. The foggy type SAED pattern reveals amorphous nature of the composite (refer supporting information Figure S5 D).

3.4 | Mechanical properties of BMI epoxy nanocomposites

Figure 7 represents the results of flexural and tensile measurements of the composites done as per ASTM standards. It is evident from the figure that for the BMI-epoxy-BTOH nanocomposites, the mechanical properties such as flexural strength and tensile strength increases with BTOH percentage reaches a maximum value at 3% and thereafter decreases. When the wt% of the BTOH nanoparticles is above a certain value, there is probability of agglomeration of nanofiller that may reduce interfacial interaction between the polymer matrix and BTOH resulting in decreased values for tensile and flexural strength.

The enhancement in the mechanical properties may be due to the surface hydroxylation of BT nanoparticles, which results in a high degree of matrix interaction and uniform dispersion of nanoparticles in the polymer matrix.[36–39] It is established from the test results that due to greater interaction between SC-EGF and the BMI-epoxy matrix there is a significant enhancement in flexural strength of BMI epoxy BTOH nanocomposites reinforced with SC-EGF compared to composites with EGF reinforcement.[40]

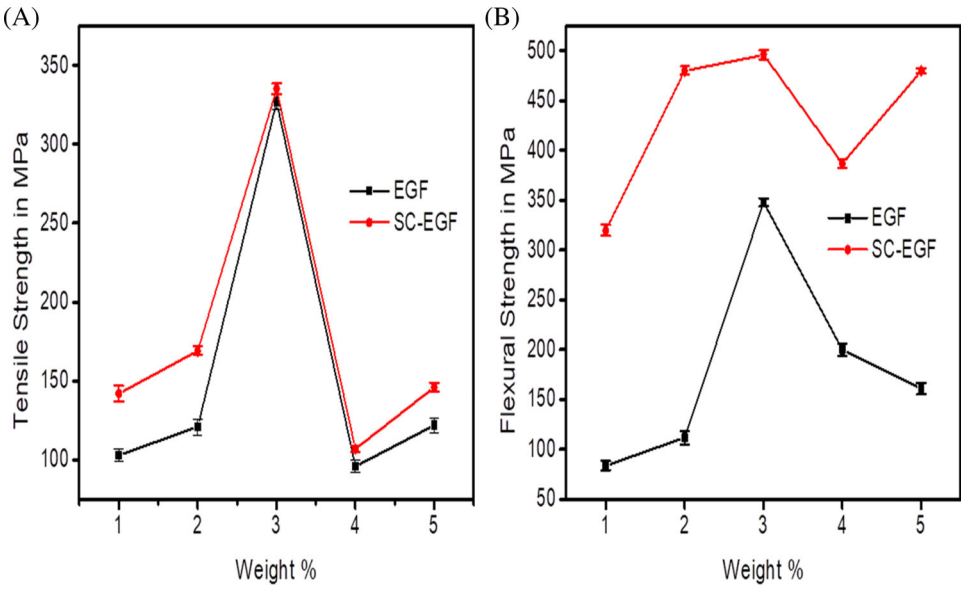

FIGURE 7 Influence of weight percentage of BTOH nanoparticles on (A) tensile strength and (B) flexural strength of the bismaleimide (BMI)-epoxy BTOH nanocomposites with E-glass fiber (EGF) and silane coupled E-glass fiber (SC-EGF) as reinforcement [Color figure can be viewed at wileyonlinelibrary.com]

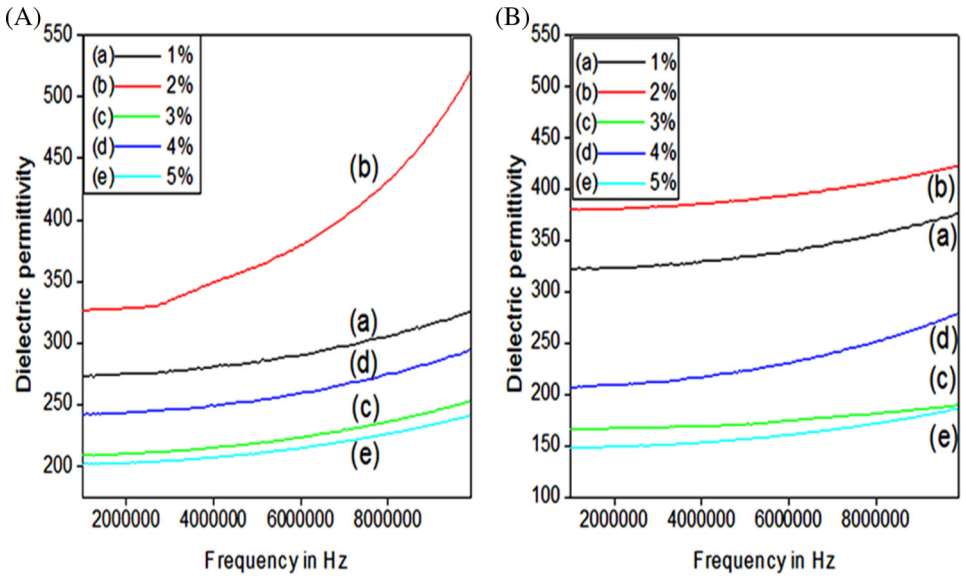

FIGURE 8 Plots of frequency versus dielectric permittivity of bismaleimide-epoxy-BTOH nanocomposites with (A) E-glass fiber (EGF) (B) silane coupled E-glass fiber (SC-EGF) as reinforcement [Color figure can be viewed at wileyonlinelibrary.com]

3.5 | Dielectric properties of the BMI-epoxy BTOH nanocomposites

3.5.1 | Dielectric permittivity

Figure 8 represents the dielectric constant versus frequency plots of BMI-epoxy-BTOH composites with different loadings of BTOH nanofiller (1%–5%). Maximum value of dielectric permittivity was obtained at 2% loading of BTOH nanoparticles in BMI-epoxy nanocomposites reinforced with SC-EGF and EGF. The functionalization of BT by surface hydroxylation improves the interfacial interaction between the BT-OH nanoparticle and the BMI-epoxy resin matrix thereby increasing the dispersion of BTOH nanofiller in the BMI-epoxy resin matrix resulting in higher dielectric constant values for the composites.[8,35,41]

3.5.2 | Dielectric loss (tan δ)

Figure 9 shows the variation of dielectric loss (tan δ) with the applied frequency for BMI-epoxy composites with differently loaded BTOH nanoparticles. Up to 2 wt% of BTOH nanoparticles, tan δ of composites remained very low.

3.5.3 | Dielectric break down strength

The characteristic breakdown strengths of BMI-epoxy-BTOH nanocomposites are illustrated in Figure 10. The energy storage capacity of polymer nanocomposites depends on the magnitude of dielectric strength. All of the MI-epoxy-BTOH nanocomposites withstand low AC

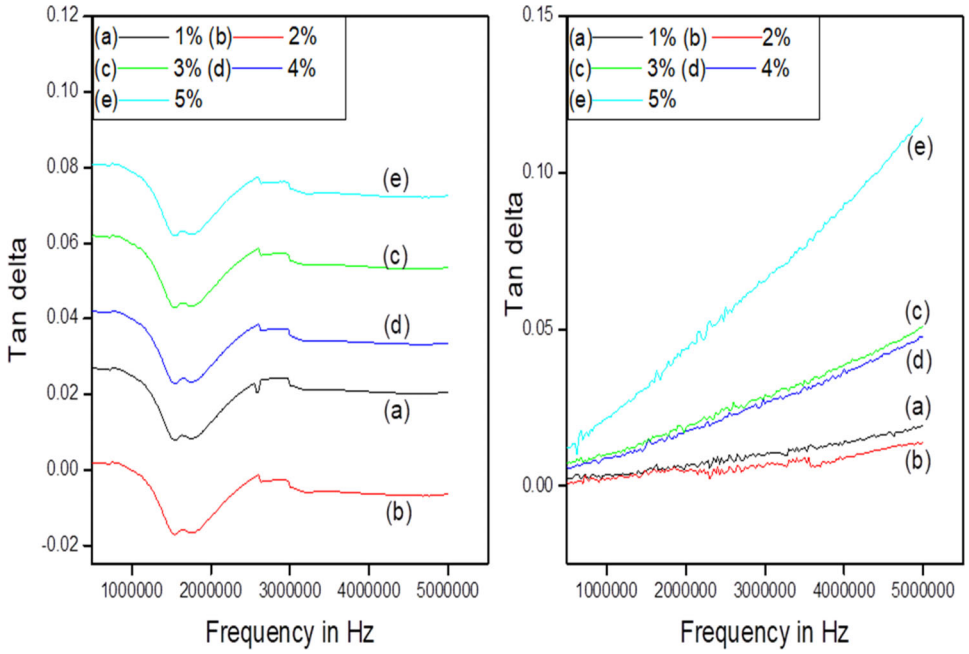

FIGURE 9 Plots of frequency-tan δ of bismaleimide-epoxy-BTOH composites with (a) E-glass fiber (EGF) (B) silane coupled E-glass fiber (SC-EGF) as reinforcement [Color figure can be viewed at wileyonlinelibrary.com]

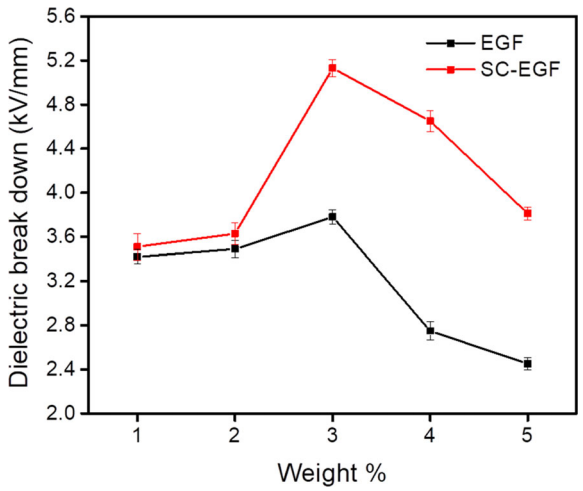

FIGURE 10 Effect of wt% of BTOH nanoparticles on dielectric breakdown strength of bismaleimide (BMI)-epoxy BTOH nanocomposites [Color figure can be viewed at wileyonlinelibrary.com]

electric field tests over 2–6 kV/mm, performed as per ASTM standard D149. At first, dielectric break down strength increases with increase in wt% of BTOH up to 3 wt% for both EGF and SC-EGF BMI-epoxy-BTOH composite which again may be due to the increased interfacial interaction and uniform distribution of nanoparticles[4,42,43] and then decreases which may be due to the nonuniform particle dispersion caused by the agglomeration of nanoparticles and voids created inside the polymer matrix.

4 | CONCLUSIONS

In our previous work, the effect of $BaTiO_3$ nanoparticles on mechanical and dielectric properties of BMI-epoxy nanocomposites was studied. Researchers report that the most effective way to strengthen the interface compatibility and enhance both mechanical and dielectric properties of the composites is the inclusion of surface modified nanofiller. A detailed comparison has been made between BMI-epoxy nanocomposites with $BaTiO_3$ (BT) nanoparticles as well as those with BTOH nanoparticles and it is found that dielectric constant, tensile strength, and flexural strength of BMI-epoxy nanocomposites with BTOH nanoparticles were increased 2, 5.15, and 2.13 times, respectively. In our present work, $BaTiO_3$ nanoparticles were synthesized by using the hydrothermal method and surface modification of $BaTiO_3$ (BT) nanoparticles using H_2O_2. XRD patterns confirm the surface hydroxylation of $BaTiO_3$ nanofillers and FTIR spectra also supports the effective surface hydroxylation. This modified BT nanoparticles (BTOH) were used to prepare glass fiber-reinforced BMI-epoxy nanocomposites with different filler loadings (1%–5%) of BTOH nanoparticles. The effect of BTOH nanoparticles on the mechanical and dielectric properties of BMI-epoxy nanocomposites was studied. The tensile strength and flexural strength of BMI-Epoxy composite 3 wt% of BTOH were increased 3.10 times and 2.21 times, respectively as compared to BMI-epoxy composite without BTOH nanofiller. The remarkable enhancement in both mechanical as well as dielectric properties may attributed

from the enhanced interfacial interaction between the polymer matrix and BTOH nanofiller and increase in BTOH filler concentration. But above a particular concentration, there is chance for filler aggregation so that uniform dispersion would not be possible, which will lead to reduction in both mechanical and dielectric properties. The synergic effect of uniform dispersion of BTOH nanofiller as well as the optimum wt% of BTOH nanofiller (3 wt%) may result in significant improvement in both mechanical and dielectric properties of BMI-Epoxy nanocomposite. Both E-glass fiber and silane coupled E-glass fiber-reinforced BMI-epoxy-BTOH nanoparticles with 3 wt% of BTOH exhibits better insulating and mechanical properties and composites with 2 wt % showed maximum dielectric constant and low dielectric loss values making this composition more suitable for high dielectric applications.

ORCID

Sunil Jose T. https://orcid.org/0000-0002-4690-1248

REFERENCES

[1] E. G. Fernandes, C. Tramidi, G. M. Di Gregorio, G. Angeloni, *Appl. Polym. Sci.* **2008**, *110*, 1606.
[2] D. Landman, in *Advances in the Chemistry and Applications of Bismaleimides BT - Developments in Reinforced Plastics—5: Processing and Fabrication* (Ed: G. Pritchard), Springer Netherlands, Dordrecht **1986**, p. 39.
[3] N. González, À. Custal, G. N. Tomara, G. C. Psarras, *Eur. Polym. J.* **2017**, *97*, 57.
[4] M. N. Almadhoun, U. S. Bhansalia, H. N. Alshareef, *J. Mater. Chem.* **2012**, *22*, 11196.
[5] T. Zhou, J. Zha, R. Cui, B. Fan, J. Yuan, Z. Dang, *ACS Appl. Mater. Interfaces* **2011**, *3*, 2184.
[6] C. Li, S. Chang, J. Lee, W. Liao, *Colloids Surf. A Physicochem. Eng. Asp.* **2010**, *361*, 143.
[7] Y. N. Hao, K. Bi, S. O'Brien, X. X. Wang, J. Lombardi, F. Pearsall, W. L. Li, M. Lei, Y. Wu, L. T. Li, *RSC Adv.* **2017**, *7*, 32886.
[8] A. Choudhury, *Polym. Int.* **2012**, *61*, 696.
[9] Y. Fan, G. Wang, X. Huang, J. Bu, X. Sun, P. Jiang, *Appl. Surf. Sci.* **2016**, *364*, 798.
[10] N. Kamezawa, D. Nagao, H. Ishii, M. Konno, *Eur. Polym. J.* **2015**, *66*, 528.
[11] X. Zhang, Y. Ma, C. Zhao, W. Yang, *Appl. Surf. Sci.* **2014**, *305*, 531.
[12] Y. Song, Y. Shen, H. Liu, Y. Lin, M. Li, C.-W. Nan, *J. Mater. Chem.* **2012**, *22*, 8063.
[13] H. W. Yujuan Niu, K. Yu, Y. Bai, F. Xiang, *RSC Adv.* **2015**, *5*, 64596.
[14] P. Kim, N. M. Doss, J. P. Tillotson, P. J. Hotchkiss, M. J. Pan, Seth R. Marder, J. Li, J. P. Calame, J. W. Perry, *ACS Nano* **2009**, *3*, 2581.
[15] S. Moharana, M. K. Mishra, B. Behera, R. N. Mahaling, *Polym. Sci. A* **2017**, *59*, 405.
[16] Y. Zhao, L. K. Seah, G. B. Chai, *Appl. Compos. Mater.* **2015**, *22*, 693.
[17] P. Hu, S. Gao, Y. Zhang, L. Zhang, C. Wang, *Compos. Sci. Technol.* **2018**, *156*, 109.
[18] Y. Kim, K. H. Kim, A. Lee, M. Kim, B. Yoo, J. Lee, *J. Nanosci. Nanotechnol.* **2017**, *17*, 5510.
[19] F. Piana, *J. Mater. Sci.* **2018**, *53*, 11343.
[20] S. Chang, W. Liao, C. Ciou, J. Lee, C. Li, *J. Colloid Interface Sci.* **2009**, *329*, 300.
[21] E. Nikita, *Eur. Phys. J. Appl. Phys.* **2015**, *69*, 10401.
[22] Y. Mao, H. Zhou, S. S. Wong, *Mater. Matters* **2010**, *5*, 50.
[23] A. Kareiva, S. Tautkus, R. Rapalaviciute, J. E. Jørgensen, B. Lundtoft, *J. Mater. Sci.* **1999**, *34*, 4853.
[24] M. Gromada, M. Biglar, T. Trzepieciński, F. Stachowicz, *Bull. Mater. Sci.* **2017**, *40*, 759.
[25] J. H. Park, D. H. Yoo, C. S. Kim, H. S. Yang, B. K. Moon, G. J. Jung, E. D. Jeong, K. S. Hong, *J. Korean Phys. Soc.* **2006**, *49*, 680.
[26] E. K. Al-Shakarchi, N. B. Mahmood, *J. Mod. Phys.* **2011**, *02*, 1420.
[27] H. Zheng, K. Zhu, Q. Wu, J. Liu, J. Qiu, *J. Cryst. Growth* **2013**, *363*, 300.
[28] K. Savitha Unnikrishnan, T. Sunil Jose, S. Dinoop lal, K. J. Arun, *Polym. Test.* **2020**, *87*, 106505.
[29] T. T. M. Phan, N. C. Chu, V. B. Luu, H. N. Xuan, D. T. Pham, I. Martin, P. Carrière, *J. Sci. Adv. Mater. Dev.* **2016**, *1*, 90.
[30] I. A. Asimakopoulos, G. C. Psarras, L. Zoumpoulakis, *Express Polym. Lett.* **2014**, *8*, 692.
[31] J. Tao, J. Ma, Y. Wang, X. Zhu, *Mater. Res. Bull.* **2008**, *43*, 639.
[32] D. Chen, Y. Luo, *J. Mater. Sci.* **1996**, *31*, 6201.
[33] C.-T. Xia, E.-W. Shi, W.-Z. Zhong, J.-K. Guo, *J. Eur. Ceram. Soc.* **1995**, *15*, 1171.
[34] P. K. Dutta, R. Asiaie, S. A. Akbar, W. Zhug, *Chem. Mater.* **1994**, *6*, 1542.
[35] D. Upc, N. González, *IEEE Trans. Dielectr. Electr. Insul.* **2017**, *24*, 2881.
[36] Y. Zhang, S. J. Park, *Polymer* **2019**, *168*, 53.
[37] S. Riaz, S.-J. Park, *Macromol. Res.* **2020**, *28*, 1116.
[38] S. Riaz, S. J. Park, *Materials* **2019**, *12*, 1354.
[39] S. H. Kim, K. Y. Rhee, S. J. Park, *Compos. B Eng.* **2020**, *192*, 107983.
[40] S. Y. Kanag, Y. K. Anandan, P. Vaidyanath, P. Baskar, *Gradjevinar* **2016**, *68*, 697.
[41] M. M. Mei Dub, W. Wanga, L. Chena, Z. Xua, H. Fua, *Polym. Plast. Technol. Eng.* **2016**, *55*, 1595.
[42] Z.-M. D. Tao Zhou, J.-W. Zha, R.-Y. Cui, B.-H. Fan, J.-K. Yuan, *ACS Appl. Mater. Interfaces* **2011**, *3,7*, 2184.
[43] Z. W. Liu Shaohui, Z. Jiwei, W. Jinwen, X. Shuangxi, *ACS Appl. Mater. Interfaces* **2014**, *6*, 1533.

SUPPORTING INFORMATION

Additional supporting information may be found online in the Supporting Information section at the end of this article.

How to cite this article: K. SU, T. SJ, S. Dl. Comparative studies of silane coupled e-glass fiber and e-glass fiber reinforced bismaleimide-epoxy hydroxylated $BaTiO_3$ nanocomposites on the dielectric and mechanical properties. *Polymer Composites*. 2021;1–9. https://doi.org/10.1002/pc.26057